Published in final edited form as:
J Chem Ecol. 2012 October ; 38(10): 1203–1214. doi:10.1007/s10886-012-0204-9.

SEAWEED ALLELOPATHY AGAINST CORAL: SURFACE DISTRIBUTION OF A SEAWEED SECONDARY METABOLITE BY IMAGING MASS SPECTROMETRY

Tiffany D. Andras[1], **Troy S. Alexander**[2], **Asiri Gahlena**[2], **R. Mitchell Parry**[3], **Facundo M. Fernandez**[2], **Julia Kubanek**[1,2], **May D. Wang**[3], and **Mark E. Hay**[1,*]

[1]School of Biology and Aquatic Chemical Ecology Center, Georgia Institute of Technology, Atlanta, GA 30332

[2]School of Chemistry and Biochemistry and Aquatic Chemical Ecology Center, Georgia Institute of Technology, Atlanta, GA 30332

[3]Wallace H. Coulter Department of Biomedical Engineering, Georgia Institute of Technology and Emory University, Atlanta, GA 30332

Abstract

Coral reefs are in global decline, with seaweeds increasing as corals decrease. Although seaweeds inhibit coral growth, recruitment, and survivorship, the mechanism of these interactions is poorly understood. Here, we used field experiments to show that contact with four common seaweeds induces bleaching on natural colonies of *Porites rus*. Controls in contact with inert, plastic mimics of seaweeds did not bleach, suggesting seaweed effects resulted from allelopathy rather than shading, abrasion, or physical contact. Bioassay-guided fractionation of the hydrophobic extract from the red alga *Phacelocarpus neurymenioides* revealed a previously characterized antibacterial metabolite, neurymenolide A, as the main allelopathic agent. For allelopathy of lipidsoluble metabolites to be effective, the compounds would need to be deployed on algal surfaces where they could transfer to corals on contact. We used desorption electrospray ionization mass spectrometry (DESI-MS) to visualize and quantify neurymenolide A on the surface of *P. neurymenioides,* and we found the molecule on all surfaces analyzed, with highest concentrations on basal portions of blades.

Keywords

Coral reefs; marine; *Phacelocarpus*; *Porites*; seaweed; seaweed-coral interactions; surface

INTRODUCTION

Coral reefs are in global decline with seaweeds commonly replacing corals. Over the last three decades, cover of live coral in the Caribbean has declined by 80% (Gardner et al., 2003), with declines of about 50% along the Great Barrier Reef in the Pacific (Bellwood et al., 2004). As corals decline, there is often a correlated increase in seaweed cover, with numerous reefs being transformed from coral-dominated, seaweed-scarce systems to coral-depauperate, seaweed-abundant systems (Mumby, 2009). Many factors have been implicated in this phase shift to algal domination (Hughes, 1994; McManus and Polsenberg, 2004; Mumby and Steneck, 2008) including overfishing (Burkepile and Hay, 2006; Hughes

*Corresponding author mark.hay@biology.gatech.edu.

et al., 2007), coral bleaching (Ostrander et al., 2000), disease (Aronson and Precht, 2001), ocean acidification (Hoegh-Guldberg et al., 2007), changing nutrient dynamics (Leichter et al., 2003), and local physical disturbances (Rogers and Miller, 2006). Many studies have investigated the factors leading to coral decline and macroalgal increases, but fewer have focused on the interactions that may maintain reefs in their degraded state, and even fewer have explored the mechanisms of these interactions.

As a result of coral-to-seaweed phase shifts, corals at all life-history stages will more frequently interact with seaweeds. Established algal communities on degraded reefs inhibit settlement and survival of coral larvae (Birrell et al., 2008a; Paul et al., 2011), suppress juvenile growth and survival (Box and Mumby, 2007), and diminish cover and survivorship of established corals (Lewis, 1986; Burkepile and Hay, 2008), creating a negative feedback that sustains reefs in their coral-depauperate states (Birrell et al., 2008b; Mumby and Steneck, 2008). In addition to documenting outcomes of seaweed-coral interactions, recent studies have suggested that mechanisms of coral decline may be chemical and microbial in nature, with an array of seaweeds and their lipid metabolites causing localized bleaching and death (Rasher and Hay, 2010; Rasher et al., 2011) as well as inducing disease and disrupting critical microbial associations in corals (Nugues et al., 2004; Smith et al., 2006; Barott et al., 2011). These results suggest that contact between algae and corals may play a significant role in enhancing coral loss and suppressing coral recovery, and that these negative interactions could be chemically mediated.

If seaweeds are transferring toxic lipids or acting as vectors of microbial pathogens, then critical interactions between seaweeds and corals will be occurring directly on, or between, organism surfaces. Surfaces represent an important site of ecological interaction because they serve as the first point of contact between two organisms and as the first line of defense in aquatic environments where organisms are constantly in contact with millions of microbial cells (Steinberg et al., 1997; Steinberg and deNys, 2002). In the case of coral-algal competition mediated by lipid-soluble metabolites that transfer to the coral following direct contact (Rasher and Hay, 2010; Rasher et al., 2011), allelopathic metabolites would need to be deployed on algal surfaces. Although previous studies have suggested surface deployment of some seaweed secondary metabolites, rigorous methods to investigate undamaged biotic surfaces in aquatic systems have remained elusive, with the majority of studies employing the “swab” or hexane “dip” methods (Schmitt et al., 1995, de Nys et al., 1998; Nylund et al., 2005; Brock et al., 2007; Nylund et al., 2010). These techniques are valuable for suggesting that target compounds may occur on surfaces, but they have limited ability to quantify compound distribution or concentration. These methods verify that cell membranes are intact after extraction or swabbing, but do not clearly establish whether intracellular compounds could be transferred without visible cell lysis . Development of a method of quantifying and evaluating the spatial distribution of secondary metabolites on biotic surfaces without submersing in solvents or mechanically contacting the cell surface would directly answer these questions.

Developments in imaging mass spectrometry allow chemical investigation of natural surfaces under ambient conditions (Takats et al., 2004; Esquenazi et al., 2009). Desorption electrospray ionization mass spectrometry (DESI-MS) has been used to localize and quantify metabolites on the surfaces of seaweeds (Lane et al., 2009; Nyadong et al., 2009), suggesting that this technique could be used to elucidate the presence and concentrations of allelopathic metabolites that may be surface deployed.

Here, we showed, based on field studies with *in situ* coral colonies, that neurymenolide A from the red alga *Phacelocarpus neurymenioides* is allelopathic to the coral *Porites rus*. DESI-MS was used to evaluate the presence, location, and approximate concentration of

neurymenolide A on the surface of live *P. neurymenioides.* This study confirms that direct contact with seaweeds can damage coral, that the majority of that damage is due to chemical rather than physical interactions, that the allelopathic metabolite is neurymenolide A, and that this compound occurs on the algal surface, allowing it to effectively transfer to and damage corals. Because neurymenolide A was first identified as an antibacterial natural product (Stout et al., 2009), this work also suggests multiple roles for deterrent compounds (Schmitt et al., 1995; Kubanek et al., 2002) located on biological surfaces where contact with multiple natural enemies (pathogens, competitors, biofoulers, consumers) will first occur, and suggests that these allelopathic metabolites could act by destabilizing the coral's microbiome by suppressing beneficial microbes, enhancing detrimental ones, or both (Ritchie, 2006; Smith et al., 2006).

METHODS AND MATERIALS

Experimental Design

To test the effects of whole algal thalli, as well as algal extracts, on coral health, we used *in situ* colonies of *Porites rus* growing at depths of 5–10 m on Votua Reef, Viti Levu, Fiji (18°13.049'S, 177°42.968'E). This coral was selected because it is abundant at the study site and is a branching coral, which makes it possible to control for genotype by simultaneously comparing multiple treatments on different branches of the same colony. Furthermore, this coral is found naturally adjacent to a variety of algae, making the study of interactions with seaweeds ecologically relevant. Ten to 12 colonies that showed no signs of bleaching and had numerous upright branches were chosen and marked with numbered tags. Four common macrophytes: the red algae *Callophycus densus, Phacelocarpus neurymenioides,* and *Plocamium pacificum,* and the green alga *Rhiphilia pencilloides* were collected from Votua Reef at depths of 5–25 m and attached directly to corals within 1 d of collection by securing the base of the alga to the base of a coral branch with a small cable tie. A plastic aquarium plant also was attached to each colony to control for shading, abrasion, and the presence of the cable tie. All treatments (i.e., the four algae plus control) were blocked by coral colony by using 10 separate colonies each with the five treatments. Damage to each coral branch was assessed after 7 d by visually assigning each treatment branch to one of four levels of bleaching. Corals that were not bleached (=0) were not visibly different relative to unmanipulated branches of the coral. Slightly bleached coral (=1) had obvious lighter coloration in the area of contact, but the tissue did not yet appear completely white and possibly dead; white, "bleached spot" coral (=2) had a bleached region that was less than the total area contacted by the alga; bleached coral (=3), was white in much of the area of contact with the alga. We had intended to assess effects on coral health using *in situ* Pulse Amplitude-Modulated (PAM) Fluorometry (Walz, Germany) to assess PSII effective quantum yield (Φ_{PSII}) of the symbiotic microalgae (zooxanthellae) living within *Porites rus*, but an instrumental error compromised readings for this part of the experiment. However, visual evaluation of bleaching is strongly correlated with assessments of effective quantum yield as measured by PAM (Rasher and Hay, 2010; Rasher et al., 2011).

Allelochemical Extraction and Isolation

All seaweeds bleached corals in areas of contact, but because a larger goal was to rigorously evaluate the surface presence of allelopathic metabolites on seaweeds, we chose to conduct follow-up bioassays only on seaweeds most amenable to surface analysis using DESI-MS. DESI-MS requires a relatively robust and planar surface that can withstand the nebulizing gas impact as well as a relatively flat surface so that mass spectral intensities will not be affected by variation in spray-surface contact geometry. This restricted further assays to *C. densus* and *P. neurymenioides* because these species have thalli that are broad, clean, and rigid enough to be good candidates for DESI-MS investigations of surface metabolites.

Quantity of each alga extracted was determined by volumetric displacement in methanol using a graduated cylinder, resulting in 100 ml samples of each species. Algae were extracted 6 times with methanol, and these crude extracts combined. Extracts were dried *in vacuo*, re-dissolved in water and ethyl acetate, and partitioned between these two solvents (250 ml each). Ethyl acetate soluble materials were dried *in vacuo* and their effects on corals tested by using methods of Rasher and Hay (2010). For each bioassay, an aliquot of ethyl acetate soluble extract equivalent to that obtained from a 10 ml volume of the alga was dissolved in 500 μl methanol and added to 196 mg Phytagel (Sigma-Aldrich, USA) and 9.5 ml of heated water; this mixture was poured over window screen and cut to create 1 cm^2 gel squares containing extract that were located at the center of a longer strip of screen, creating a "band-aid" like strip with gel squares in the center. Control gel strips were made with an identical procedure, but contained only the solvent. Strips were attached to corals by wrapping them around a coral upright and fastening this loosely with a cable tie. Treatments were again blocked by colony so that each colony (N= 12) contained a strip with the extract from each alga and a control strip. Coral health was assessed after 24 h using PAM Fluorometry conducted at the approximate center of each gel strip. Although it is possible that a single coral colony in contact with each of several seaweeds (the experiment above) or each of the different chemical fractions tested here could experience a synergistic effect of these multiple treatments/colony, all visible or PAM measured effects that we have been able to document over short periods in these, or previous, experiments (Rasher and Hay 2010, Rasher et al. 2011) occurred only at areas of direct algal or extract contact. We, therefore, chose to minimize among coral variance by blocking our treatments by colony rather than leaving among-individual variance unaccounted for by putting each individual replicate of all treatments on separate colonies. Gel strips were deployed and PAM data were collected at low tide to avoid dangerous current in the channel where assay corals were common; safety concerns in this habitat necessitated daytime PAM readings instead of dark-adapted readings at night.

Because initial tests of crude extracts demonstrated that extracts of *P. neurymeniodes* were more potent than those of *C. densus*, we conducted further bioassay-guided separation experiments with *P. neurymenioides* to separate, purify, and identify allelopathic metabolites. Fractions produced by all of the below separations were tested in the field using the gel-based procedures of Rasher et al. (2011) described above (N=9–12). We extracted an additional 200 ml volume of *P. neurymenioides* with 100% MeOH (repeated 3 times and combined) followed by 50:50 MeOH: dichloromethane (repeated 4 times and combined with the methanol extract). This crude extract was dried *in vacuo* and then liquid-liquid partitioned between equal volumes of hexane and 9:1 MeOH: H_20 (500 ml each). A 20 ml equivalent of each partition was dried *in vacuo* for testing in the field. The remaining 9:1 MeOH: H_20 portion then was further fractionated by partitioning with equal volumes of chloroform and 3:2 MeOH: H_20 (800 ml each) and both were dried *in vacuo* with a 20 ml equivalent aliquot separated for field tests. The chloroform-soluble partition was fractionated further via bench-top chromatography. Fractionation was achieved on 160 g silica gel via a step gradient from 100% hexane to 100% ethyl acetate, with a final flush of 93:5:2 ethyl acetate : methanol : acetic acid. The 28 resultant 100 ml fractions were recombined into 6 fractions (F1–F6) based upon similarity as observed by TLC.

Fractions that decreased effective quantum yield were analyzed using highperformance liquid-chromatography mass-spectrometry (HPLC-MS) and normal-phase high-performance liquid chromatography (HPLC) as described inStout et al. (2009). All active fractions contained the same prominent peaks: a pair of peaks relating to the interchangeable atropisomers of neurymenolide A followed immediately by a single peak of neurymenolide B (Stout et al., 2009). Accurate identification of compounds was confirmed by using a combination of methods including: comparison with known ^1H NMR spectra, retention time

and peak shape by LC-MS and/or HPLC, and mass measurements using ESI-time-of-flight (TOF) MS accurate to 1 ppm in positive ion mode. For all of these methods, NMR chemical shifts and coupling constants and molecular ions measured by MS matched reported data for neurymenolide A (Stout et al., 2009)

After demonstrating that neurymenolides were present in fraction 4 (generated from the 80:20 and 50:50 hexane;ethyl acetate elutions) from the silica chromatography of the original chloroform partition, we used normal-phase silica HPLC (employing a gradient of hexanes and ethyl acetate on a 250×9.4 mm 5 μm Agilent RX-SIL column) to yield pure neurymenolide A, pure neurymenolide B, and the "remainder" of natural products in this fraction. A 500 μl sample of fraction 4 extract at a concentration of 20 mg/ml in 80:20 hexanes: ethyl acetate was injected for purification (repeated 12 times for purification of a 15 ml equivalent). HPLC separation was achieved using a flow rate of 3 ml/min in a solvent gradient from 50:50 hexanes: ethyl acetate to 100% ethyl acetate to 100% hexanes and back to initial starting conditions over the course of a 37 min run. Peaks were visualized using UV absorption at 270 nm. Field bioassays of these metabolites and of the "remainder" were conducted as described above (N=10).

Desorption Electrospray Ionization Mass Spectrometry (DESI-MS)

The above assays identified neurymenolide A as the single allelopathic compound in *P. neurymeniodes.* To evaluate whether neurymenolide A was present on the surface of *P. neurymenioides* and at what concentrations, living thalli of *P. neurymenioides* were flown from Fiji to Atlanta and held in recirculating aquaria. DESI-MS was performed under ambient conditions using a living blade immediately after removal from the plant and with no pretreatment. For the evaluation, we used a custom-built DESI ion source (Nyadong et al., 2009) mounted on an LCQ DECA XP+ quadrupole ion trap mass spectrometer (Thermo Finnigan). Experiments were performed using a solvent spray solution of 100 μM NH_4Cl (Sigma-Aldrich) in MeOH at a flow rate of 7 m1/min. The nebulizer gas pressure was set to 120 psi. The ion transfer capillary was held at 300 °C, and experiments were performed in the negative ion mode. The DESI sprayer emitter was positioned 2 mm above the algal surface at an angle of 55°. Data were collected in full scan mode (m/z 150–500) using Xcalibur software version 2.0 (Thermo Finnigan). The automatic gain control (AGC) was disabled with a fixed ion injection time of 40 ms.

Imaging data were acquired in looped scanning mode, the sampling stage being controlled by LabVIEW (National Instruments). Samples were probed with a scan speed in both x and y dimensions of 160 μm/s and a step size in the y-dimension of 180 μm. Images were processed with "omniSpect", an in-house web-based MATLAB (version R2010b, MathWorks) script that allowed converting large RAW (Thermo) mass spectral data files to CDF format and the subsequent creation of molecular images using a remote server for faster data processing. The details of this system are available at http://omnispect.bme.gatech.edu.

Compound Distribution Across Algal Surfaces

Distributions of neurymenolide A across surfaces from different portions of thalli were assessed by cutting 2 squares of approximately 0.5 cm^2 from the top, middle, and bottom of five separate 7.0–10.0 cm tall blades of *P. neurymenioides*. Squares were mounted to a glass slide using fast-drying glue, and mass spectral data were collected for 100 scans per square. The total ionic intensity of neurymenolide A was summed (using both the $[M\text{-}H]^-$ and $[M+Cl]^-$ signals) within a square and averaged for the two sub-samples at each location for that blade, producing an average intensity for top, middle, and bottom sections for each of the 5 independent blades. In order to determine whether the compound was differentially

distributed at edges or centers of blades, data were collected from the center, with the midrib avoided, and one side of 4 separate blades (1.0–2.5 cm broad blades) for a duration of 50 scans and averaged as above. Analyses of chronograms and spectra were conducted using QualBrowser software (Thermo).

DESI-MS imaging data also were collected using algal samples (0.5–2.0 cm length; 0.2–2.0 cm width) taken fresh from seawater tanks and attached, without pretreatment, to a microscope slide with instant adhesive glue. Blades used for these images were small, adventitious branches arising from the midrib of larger blades. Algal cell integrity was verified before and after DESI-MS experiments by evaluation under a light microscope.

Estimation of Surface Concentrations

Surface concentrations of neurymenolide A were estimated by comparing integrals of natural surface concentrations to a standard curve generated on the same day by depositing 5 μl aliquots of neurymenolide A dissolved in ethyl acetate at known concentrations (1 mM, 100 μM, 10 μM, 1 μM) onto a PTFE substrate. Absolute concentrations of standards were calculated by dividing the total number of moles deposited by the area over which the sample was observed to spread (r = 2 mm), resulting in absolute concentrations of 300 to 0.3 pmol/mm^2, respectively. The summed ionic intensity for each concentration of neurymenolide A was calculated using the method described above for distribution on large blades. Concentration was then plotted as a function of summed intensity in order to estimate concentrations from intensity values on sample surfaces (Supplemental Fig. 1). Average concentration of neurymenolide A on the surface of live seaweeds was estimated using the calibration plot by averaging 3 randomly chosen spots from the DESI-MS chemical image of a single algal blade.

Statistics

Whole algal pairings with corals were evaluated using a *paired sign test* for each treatment against the control. A Bonferroni correction setting $\alpha = 0.012$ corrected for using the control value in multiple contrasts (contrasts of control vs. treatments for four total comparisons).

Data from all extract-coral pairings were tested using an *ANOVA* blocked by coral colony. Data for the first three experimental pairings adhered to assumptions of a parametric test without transformation, and data from the last set of treatments were square root transformed to reach normality. *Post-hoc Tukey tests* were completed for pair-wise comparisons between treatments and against the control. An *ANOVA* blocked by blade contrasted metabolite concentrations on top, middle, and bottom portions of blades. This was followed by *post-hoc Tukey tests*. A *paired T-test* evaluated data from edge vs. center sections of blades.

Purification of Oxidized Neurymenolide A

Fractions 5 and 6 generated during benchtop silica fractionation of the chloroform-soluble partition were combined, and one oxidized neurymenolide metabolite was purified using the same HPLC system and column as for neurymenolides A and B. A 30-minute gradient from 50:50 hexane: ethyl acetate to 100% ethyl acetate was used, with diode-array detection at 295 nm. The material was dissolved at 10 mg/ml in 50:50 hexane:ethyl acetate and injected in 500 μl aliquots to yield 150 μg of pure compound. Several other peaks with the same mass and λ_{max} were observed, but could not be separated using this solvent system.

NMR analysis

All ^{1}H and ^{13}C NMR spectra were collected on a Bruker DRX-500 instrument equipped with a 5 mm broadband probe, using the standard pulse sequences. A $CDCl_3$ solution of the

oxidized neurymenolide product in a Shigemi tube was analyzed using the solvent residual peak as an internal standard ($CHCl_3$ ^1H = 7.26 ppm, ^{13}C = 77.16 ppm). NMR solvents were purchased from Cambridge Isotope Laboratories.

RESULTS

Effects of Live Algae

All four species of algae produced significant levels of coral bleaching when placed in contact with branches of *P. rus* ($N = 9$) for seven days in the field (Fig. 1A; $P =< 0.001$ to 0.009 for all contrasts; *paired sign test* each treatment vs. the control, = 0.012 to control for multiple comparisons). Levels of bleaching tended to be greater for the red alga *P. pacificum* and the green alga *R. penicilloides* than for the red algae *C. densus* and *P. neurymenioides*. Contact with a plastic algal mimic (the control for contact, shading, abrasion, etc.) caused no bleaching. Bleaching for all pairings occurred only in areas of direct contact. Because *C. densus* and *P. neurymenioides* were morphologically most amenable to DESI-MS analysis, we focused investigation of allelopathy on these species.

Allelochemical Pairings

When crude extracts from *C. densus* and *P. neurymenioides* were bioassayed *in situ* against *P. rus* ($N = 12$), there was a significant effect of treatment, but not colony (Fig. 1B; *blocked ANOVA* $F_{2, 22} = 9.02$, $P < 0.001$ for treatment and $F_{11, 22} = 0.40$, $P = 0.948$ for colony). The extract from *P. neurymenioides* decreased the effective quantum yield values of the coral by 41% (*Post-hoc Tukey test,* $P < 0.01$) in 24h; the extract from *C. densus* had no effect. Visual bleaching beneath extract strips occurred for 10 of 12 *P. neurymenioides* replicates, 2 of 12 *C. densus* replicates, and 0 of 12 control replicates.

The crude extract of *P. neurymenioides* was reassessed along with fractions of the crude extract generated from solvent partitions. In this assay, there was a significant effect of both treatment and colony (Fig. 2A; *blocked ANOVA* $F_{4, 32} = 11.38$, $P < 0.001$ for treatment and $F_{8, 32} = 3.33$, $P = 0.007$ for colony). The crude extract and chloroformsoluble fraction of that extract both decreased effective quantum yield with respect to control values ($P < 0.001$, and $P = 0.007$, respectively, *Post-hoc Tukey tests*); the hexane and more polar fractions of the crude extract had no significant effects.

When the active, chloroform-soluble fraction was fractionated via normal phase chromatography and fractions tested against coral in the field, treatment, but not colony, had a significant effect (Fig. 2B; *blocked ANOVA* $F_{5, 40} = 10.54$, $P < 0.001$ for treatment and $F_{9, 40} = 1.36$, $P = 0.233$ for colony). Fraction 4 decreased effective quantum yield by 45% ($P < 0.001$, *Post-hoc Tukey test*), with all other fractions being inactive. Preliminary evaluations of both active fractions (chloroform and chloroform F4) were conducted by LC-MS before further purification. Retention times (not shown but compared to Stout et al., 2009) and *m/z* values (Fig. 3A) indicated the presence of neurymenolides in both fractions. From the chloroform F4 fraction, pure neurymenolide A and neurymenolide B were obtained using normal-phase HPLC (Fig. 3B). Purity of both compounds was confirmed using an ESI-TOF mass spectrometer (Fig. 3C).

Tests of the separate components from fraction 4 (F4) (*blocked ANOVA* $F_{3, 27} = 13.88$, $P < 0.001$ for treatment and $F_{9, 27} = 1.27$, $P = 0.295$ for colony) demonstrated that neurymenolide A was solely responsible for the allelopathic effects of the F4 fraction, suppressing effective quantum yield by 35% (Fig. 2C; $P < 0.001$, *Post-hoc Tukey test*). Neurymenolide B and "remainder" portions of F4 had no detectable effect.

Desorption Electrospray Ionization Mass Spectrometry

DESI-MS conducted on mature blades from *P. neurymenioides* revealed that the older, lower portions of the blades contained surface concentrations of neurymenolide A that were more than double the concentrations occurring on the top or middle portions (Fig. 4A; *blocked ANOVA* $F_{2, 8} = 4.91$, $P = 0.041$ for treatment and $F_{4, 8} = 1.61$, $P = 0.262$ for blade). Concentration did not differ between edges and centers of blades (Fig. 4B; *paired T-test* $P = 0.234$). DESI-MS imaging was performed on a young, adventitious blade sprouting from the midrib of a mature blade (Fig. 5A). This chemical image shows a nearly uniform distribution of neurymenolide A across the surface of the small blade with a few areas of increased concentration (Fig. 5B). Ion masses consistent with singly and doubly oxidized neurymenolide A also were observed on the surface in an intensity nearly matching that of neurymenolide A (Fig. 5C). When these compounds were color-coded by class with neurymenolide A pink and the degradation products green, an overlay of both images (Fig. 5D) produced a purple color. This overlay shows the location of neurymenolide A and its degradation products to be similar across the surface.

The presence of singly oxidized neurymenolide A was confirmed by purification and NMR spectroscopy. The identity of the mass signal tentatively identified as doublyoxidized neurymenolide A was not confirmed. LC-MS analysis of the chloroform fraction of the *P. neurymenioides* extract shows a series of broad, overlapping peaks with the same λ_{max} as neurymenolide A at 295 nm, and an $[M+H]^+$ *m/z* of 385, corresponding with a molecular formula of $C_{24}H_{32}O_4$, i.e., neurymenlide A plus one oxygen. To confirm this, a single peak was isolated by normal phase semi-preparative HPLC to yield approximately 150 μg pure compound. NMR spectral analysis shows that, like neurymenolide A, this compound has a pyrone ring and 4 olefins. However, this compound has one less R_2CH_2 and a new R_2CHOH ($\delta_C = 70.4$ ppm, $\delta_H = 4.33$ ppm). The OH ^1H signal was not observed, as it likely overlaps with the residual water peak. The full NMR data are:

^{13}C NMR: 165.7, 164.7, 164.3, 137.5, 133.3, 131.6, 130.9, 129.6, 129.1, 125.9, 124.7, 106.3, 102.2, 70.4, 36.8, 35.3, 34.3, 30.2, 28.3, 26.2, 24.0, 21.8, 20.7, 14.4 ppm. ^1H NMR ppm, integrations, multiplicity (*J* in Hz): 6.71, 1H, s; 6.38, 1H, ddt (15.4, 10.6, 1.3); 6.15, 1H, ddd (10.6, 10.6, 2.3); 5.84, 1H, s; 5.73, 2H, m; 5.67, 2H, m; 5.44, 1H, dtt (10.7, 7.2, 1.6); 5.31, 1H, dt (10.7, 7.3, 1.4); 4.78, 1H, m; 4.33, 1H, m; 2.79, 2H, m; 2.64, 1H, dt (13.8, 4.2); 2.16, 1H, ddd (13.8, 8.9, 6.8); 2.02, 2H, pd (7.2, 1.4); 1.68, 2H, m; 1.62, 1H, m; 1.57, 1H, m; 1.38, 1H, m; 1.26, 1H, m; 1.15, 1H, m; 0.95, 1H, m; 0.94, 3H, t (7.2); 0.78, 1H, m.

Peak intensities from DESI-MS images were converted semi-quantitatively to concentration of neurymenolide A on the surface using a calibration plot (Supplemental Fig. 1). The majority of locations on the surface of *P. neurymenioides* show intensities of Neurymenolide A between 1.5 X 10^5 and 3 X 10^5 (arbitrary units) giving an average surface concentration of 300 +/− 200 pmol/mm^2 across the surface of small, young blades, which matches the approximate concentrations at the tops and middles of larger blades. Additionally, however, some locations on the algal surface show intensities of neurymenolide A as high as 3 X 10^5, corresponding to approximate concentrations of 800 pmol/mm^2.

DISCUSSION

Contact with all four species of reef algae produced bleaching on natural colonies of *Porites rus* growing in the field; the plastic algal mimic produced no bleaching. The green algae *R. penicilloides* and the red algae *P. pacificum* caused severe bleaching, while the red algae *P. neurymenioides* and *C. densus* caused significant but less severe bleaching (Fig. 1A). In addition, visible patterns of bleaching by algal extracts appear to be related to effects on photosynthesis as crude extract of *P. neurymenioides* caused both higher incidence of

bleaching and significantly lower effective quantum yield values than did extracts of *C. densus*. Recent studies have shown several macrophytes to cause bleaching and sometimes death in multiple species of corals (Rasher and Hay, 2010; Rasher et al., 2011). Past studies have focused on interactions on shallow reef-flats utilizing small coral branches. Our study produced similar results using seaweeds typical of deeper waters (3–50 m depths) on deeper-water corals that were *in situ* and not fragmented. Given that all four of the seaweeds tested caused bleaching of established coral colonies, that the plastic control plant caused no bleaching or other signs of damage to the coral, and that even the modest bleaching and 41% decrease in effective quantum yield caused by *P. neurymenioides* was due to allelopathic effects of neurymenolide A, allelopathic algal-coral interactions appear common in deeper, as well as shallow (Rasher and Hay, 2010; Rasher et al., 2011), reef systems. This indicates algal-coral competition, and algal allelopathy in particular, could have a substantial impact on coral decline and on suppression of coral recovery, especially on modern reefs where corals are less abundant, seaweeds more abundant, and thus seaweed-coral contacts more frequent. Because all assessments were made by blocking each of our multiple treatments by coral colony (i.e., all treatments were applied to each of several independent colonies), we cannot exclude the possibility that effects of treatments on one branch could cause photosynthetic changes in other branches. However, in this and previous experiments (Rasher and Hay, 2010, Rasher et al., 2011) initial effects on visual bleaching and effective quantum yield have been restricted to only those sites of direct contact with specific treatments – suggesting that branches function independently over this spatial and temporal scale. Additionally, through multiple rounds of testing in assays reported here, only single treatments decreased effective quantum yield, and we were easily able to follow this activity to a single algal compound. These patterns suggest that synergistic effects are unlikely.

Hydrophobic crude extracts of *P. neurymenioides* reproduced bleaching patterns seen in assays using the whole alga, with bleaching occurring in 10 of 12 replicates in the former and 7 of 9 in the latter (Fig. 1B). Although many bioactive secondary metabolites have been isolated from *C. densus*, with several of these exhibiting antibacterial and antifungal activities (Kubanek et al., 2005, 2006; Lane et al., 2007, 2009), extracts from this alga did not significantly suppress photosynthesis or cause bleaching in corals. It is possible that compounds from this alga are not allelopathic, or that our bioassay methods degraded allelopathic compounds from this alga. The latter seems unlikely given that the major secondary metabolites in *C.* densus are more stable than the neurymenioides under laboratory conditions (J. Kubanek pers. obs.) and that our bioassay methods worked well with extracts form *P. neurymenioides* and numerous other seaweeds (Rasher and Hay, 2010; Rasher et al., 2011).

When the lipid-soluble extract of *P. neurymenioides* was partitioned and tested in the field, both the crude extract and the chloroform-soluble fraction significantly decreased effective quantum yield; other fractions had no detectable effects. Coral colony did have a significant effect, indicating variance among coral individuals in the magnitude of response to contact with algae or algal metabolites. Further fractionation and purification of the active chloroform-soluble extract from *P. neurymenioides* indicated that only neurymenolide A was allelopathic to our test coral (Fig. 2). There was a non-significant suggestion of activity in the hexane-soluble fraction (Fig. 2A), but traces of neurymenioide A occurred in this fraction (Supplemental Fig.2), suggesting that it could have generated this trend.

Given that considerable contact between seaweeds and corals occurs on natural reefs following loss of herbivores (Lewis, 1986; Hughes et al., 2010), and that this has occurred only in recent years due to overharvest of reef herbivores (Jackson et al., 2001), it seems doubtful that neurymenolide A was selected for allelopathy against corals. Instead, the large numbers of algal natural products that suppress herbivores or microbes and the long and

important role these enemies have played in seaweed biology (Hay and Fenical, 1988; Engel et al., 2002; Kubanek et al., 2003; Hay, 2009) combined with the potency of neurymenolide A against methicillin-resistant *Staphylococcus aureus* (Stout et al., 2009) suggests that neurymenolide A may have evolved due to its protective function against consumers or pathogens, but is fortuitously also allelopathic to coral. It, therefore, is possible that rather than directly poisoning corals, neurymenolide A could act by disrupting protective bacteria, or enhancing pathogenic bacteria associated with coral mucus (Ritchie, 2006) as suggested by some previous observations of coralseaweed interactions (Nugues et al., 2004; Smith et al., 2006; Barott et al., 2011).

Despite previous studies showing seaweeds to be allelopathic to corals, the localization of natural products and the means of transfer from seaweeds to corals have remained uncertain. Methods such as hexane dipping (de Nys et al., 1998) and physical swabbing of surfaces (Schmitt et al., 1995) have suggested that allelopathic compounds occur on surfaces where they could transfer to corals (Rasher and Hay, 2010; Rasher et al., 2011); however, DESI-MS imaging allows chemical investigation of natural surfaces with minimal handling, thus improving our confidence that substances are on surfaces rather than in seaweeds. We focused on a species whose flat surface was especially amenable to investigations by DESI-MS. Surface investigations of more harmful seaweeds such as *R. penicilloides* and *P. pacificum* would be desirable, but their delicate (*P. pacificum*) or filamentous (*R. penicilloides*) surfaces make this challenging for investigation by DESI-MS, and may require other techniques such as imaging of blots from algal surfaces (Ifa et al., 2011). However, patterns of bleaching for these algae vs. the plastic control suggest that chemical suppression of coral health has occurred for those species, as suggested by other investigations as well (Jompa and McCook, 2003; Rasher et al., 2011).

Neurymenolide A was found on all surfaces of *P. neurymenioides* (Fig. 5B). The average concentration on older, bottom portions of blades was more than double the concentration found on younger tissues. Although this may suggest that neurymenolide A is being sequestered in older tissues, thus defending basal portions that anchor the entire seaweed, it is also possible that the natural product simply accumulates in tissues over time or is selectively allocated to older tissues as these have experienced longer-term exposure to microbial enemies. Neurymenolide A and all other chemical extracts were tested at approximately natural, whole tissue concentrations by extracting 10 ml volumes of algae and placing these extracts, or fractions from these, into 10 ml volumes of gel. While the concentration of neurymenolide A detected by DESI-MS is low, in only the hundreds of pmol/mm^2 range, previous studies have also detected surface concentrations for bioactive secondary metabolites in this range and have shown these compounds to be active at those concentrations (Lane et al., 2009). Additionally, the antibacterial activity of neurymenolide A has an IC_{50} of 2.1 μg/ml (Stout et al., 2009) suggesting that the low concentration detected by DESI-MS could be ecologically active. When neurymenolide A is placed into our gels for assays, the compound is presumably distributed throughout the gel, rather than concentrated on its surface (potentially limiting its surface concentration). However, when in the field in Fiji, where we test extract effects, we are unable to conduct careful quantitative chemistry, so the question of how metabolites are distributed in, on, or diffuse through the gel remains unresolved.

In addition to neurymenolide A, oxidative degradation compounds were also detected in extracts and on natural surfaces, These degradation products occurred in not only similar distribution relative to neurymenolide A (Fig. 5D) but also in similar intensity on the surface of *P. neurymenioides* (Fig. 5D), suggesting oxidation may occur rapidly for this metabolite. Though oxidation of compounds may occur as a by-product of electrospray ionization processes, these ion masses were not observed when pure neurymenolide standards were

subject to DESI-MS, suggesting the appearance of these compounds on natural surfaces is due to biological oxidation rather than a methodological artifact.

DESI-MS allows chemical investigation of natural surfaces, having the potential to elucidate distribution and concentration of chemicals across whole tissue surfaces (Esquenazi et al., 2008). Although some natural products have been shown to be associated with particular structural features of an organism's surface (Lane et al., 2009), DESI-MS can also reveal these sorts of associations by comparing and overlaying chemical images and optical images of the physical surface. These recent developments in imaging mass spectrometry technology have provided a new stepping-stone in the study of interactions at organism's surfaces. Especially in aquatic environments where organisms are constantly in contact with millions of microbes per milliliter seawater, understanding the roles that chemicals play on biotic surfaces is key to understanding microbe-host, host-epibiont, competitive, and plant-grazer interactions.

Although debate has continued surrounding the leeching of organic compounds into seawater (Dobretsov et al., 2006), this study conclusively demonstrates that lipid-soluble compounds with antibacterial and allelopathic effects can be deployed on the surfaces of algae. The bleaching localized to sites of direct contact with algae seen in this as well as prior studies combined with presence of active allelopathic metabolites on the surface of a damaging alga suggest direct contact with algae may be more important to the outcome of algal-coral competition than leeching alone.

Despite persistent obstacles in reef management, understanding that allelopathic algal-coral interactions occur under direct contact has implications for reef management. Removal of algal communities in close proximity to established coral colonies should be a focus of reef restoration. Herbivore grazing is a large and consistent means of removing algae from reefs (Lewis, 1986; Hughes et al., 2007; Burkepile and Hay, 2008, 2009), thereby preventing further reef degradation by removing algal competitors and increasing substrate availability for coral recruitment and growth. Reef management might profit from an enhanced understanding of which seaweeds pose the greatest threat to corals, which herbivores most control those seaweeds, and focusing efforts on synergistic strategies of seaweed suppression and herbivore protection in order to best facilitate coral recovery. Given our imperfect knowledge of seaweed-coral interactions, a reasonable immediate strategy is to focus on increasing herbivore species richness, which decreases overall algal abundance due to feeding complementarity (Bellwood et al., 2003, 2006; Burkepile and Hay, 2008; Hoey and Bellwood, 2009; Rasher and Hay, unpublished) and aids in the recovery status of reefs (Ledlie et al., 2007).

Supplementary Material

Refer to Web version on PubMed Central for supplementary material.

Acknowledgments

We thank the Fijian government and the Korolevu-i-wai district elders for granting research permissions, C. Dell, A. Warneke, D. Gibbs, and A. Hoey for field help, and V. Bonito for scientific and cultural insight in Fiji. Support came from the National Science Foundation (OCE 0929119), the National Institutes of Health (U01-TW007401), and the Teasley Endowment to the Georgia Institute of Technology. FMF acknowledges support from ARRA NSF MRI Instrument Development grant #0923179.

REFERENCES

Aronson RB, Precht WF. White-band disease and the changing face of Caribbean coral reefs. Hydrobiologia. 2001; 460:25–38.

Barott KL, Rodriguez-brito B, Janouskovec K, Marhaver JL, Smith JE, Keeling P, Rohwer FL. Microbial diversity associated with four functional groups of benthic reef algae and the reef building coral Montastrea annularis. Environ. Microbiol. 2011; 13:1192–1204. [PubMed: 21272183]

Bellwood DR, Hoey AS, Choat JH. Limited functional redundancy in high diversity systems: resilience and ecosystem function on coral reefs. Ecol. Lett. 2003; 6:281–285.

Bellwood DR, Hughes TP, Falke C, Nystrom M. Confronting the coral reef crisis. Nature. 2004; 429:827–833. [PubMed: 15215854]

Bellwood DR, Hughes TP, Hoey AS. Sleeping functional group drives coral-reef recovery. Curr. Biol. 2006; 16:2434–2439. [PubMed: 17174918]

Birrell CL, Mccook LJ, Willis BL, Harrington L. Chemical effects of macroalgae on larval settlement of the broadcast spawning coral Acropora millepora. Mar. Ecol. Prog. Ser. 2008a; 362:129–137.

Birrell CL, Mccook LJ, Willis BL, Diaz-pulido GA. Effects of benthic algae on the replenishment of corals and the implications for the resilience of coral reefs. Oceanogr. Mar. Biol. Annu. Rev. 2008b; 46:25–64.

Brock E, Nylund GM, Pavia H. Chemical inhibition of barnacle larval settlement by the brown alga Fucus vesiculosa. Mar. Ecol. Prog. Ser. 2007; 337:165–174.

Box SJ, Mumby PJ. Effect of macroalgal competition on growth and survival of juvenile Caribbean corals. Mar. Ecol. Prog. Ser. 2007; 342:139–149.

Burkepile DE, Hay ME. Herbivore vs. nutrient control of marine primary producers: context-dependent effects. Ecology. 2006; 87:3128–3139. [PubMed: 17249237]

Burkepile DE, Hay ME. Herbivore species richness and feeding complementarity affect community structure and function on a coral reef. Proc. Natl. Acad. Sci. U.S.A. 2008; 105:16201–16206. [PubMed: 18845686]

Burkepile DE, Hay ME. Nutrient versus herbivore control of macroalgal community development and coral growth on a Caribbean reef. Mar. Ecol. Prog. Ser. 2009; 389:71–84.

De nys R, Dworjanyn SA, Steinberg PD. A new method for determining surface concentrations of marine natural products on seaweeds. Mar. Ecol. Prog. Ser. 1998; 162:79–87.

Dobretsov S, Dahms HU, Harder T, Qian PY. Allelochemical defense against epibiosis in Caulerpa recemosa var turbinate. Mar. Ecol. Prog. Ser. 2006; 318:165–175.

Engel S, Jensen PR, Fenical W. Chemical ecology of marine microbial defense. J. Chem. Ecol. 2002; 28:1971–1985. [PubMed: 12474894]

Esquenazi E, Coates C, Simmons L, Gonzalez D, Gerwick WH, Dorrestein PC. Visualizing the spatial distribution of secondary metabolites produced by marine cyanobacteria and sponges via MALDI-TOF imaging. Mol. Biosys. 2008; 4:562–570.

Esquenazi E, Dorrestein PC, Gerwick WH. Probing marine natural product defenses with DESI-imaging mass spectrometry. Pro. Natl. Acad. Sci. U.S.A. 2009; 106:7269–7270.

Gardner TA, Cote IM, Gill JA, Grant A, Watkinson AR. Long-term region-wide declines in Caribbean corals. Science. 2003; 301:958–960. [PubMed: 12869698]

Hay ME, Fenical W. Marine plant-herbivore interactions: The ecology of chemical defense. Annu. Rev. Ecol. Sys. 1988; 19:111–145.

Hay ME. Marine chemical ecology: Chemical signals and cues structure marine populations, communities, and ecosystems. Annu. Rev. Mar. Sci. 2009; 1:193–212.

Hoegh-guldberg O, Mumby PJ, Hooten RJ, Steneck OS, Greenfield P, Gomez E, et al. Coral reefs under rapid climate change and ocean acidification. Science. 2007; 318:1737–1742. [PubMed: 18079392]

Hoey AS, Bellwood DR. Limited functional redundancy in a high diversity system: Single species dominates key ecological process on coral reefs. Ecosystems. 2009; 12:1316–1328.

Hughes TP. Catastophies, phase-shifts, and large-scale degradation of a Caribbean coral-reef. Science. 1994; 265:1547–1551. [PubMed: 17801530]

Hughes TP, Rodrigues MJ, Bellwood DR, Ceccarelli D, Hoegh-guldberg O, Mccook L, et al. Phase shifts, herbivory, and the resilience of coral reefs to climate change. Curr Biol. 2007; 17:360–365. [PubMed: 17291763]

Hughes TP, Graham NAJ, Jackson JBC, Mumby PJ, Steneck RS. Rising to the challenge of sustaining coral reef resilience. Trends Ecol. Evol. 2010; 25:633–642. [PubMed: 20800316]

Ifa DR, Srimany A, Eberlin LS, Naik HR, Bhat V, Cooks RG, Pradeep T. Tissue imprint imaging by desorption electrospray ionization mass spectrometry. Anal. Methods. 2011; 3:1910–1912.

Jackson JBC, Kirby MX, Berger WH, Bjorndal KA, Botsford LW, Bourque BJ, et al. Historical overfishing and the recent collapse of coastal ecosystems. Science. 2001; 293:629–638. [PubMed: 11474098]

Jompa J, Mccook LJ. Coral-algal competition: macroalgae with different properties have different effects on corals. Mar. Ecol. Prog. Ser. 2003; 258:87–95.

Kubanek J, Whalen KE, Engel S, Kelly SR, Henkel TP, Fenical W, Pawlik JR. Multiple defensive roles for triterpene glycosides from two Caribbean sponges. Oecologia. 2002; 131:125–136.

Kubanek J, Jensen PR, Keirfer PA, Sullards MC, Collins DO, Fenical W. Seaweed resistance to microbial attack: A targeted chemical defense against marine fungi. Proc. Natl. Acad. Sci. U.S.A. 2003; 100:6916–2921. [PubMed: 12756301]

Kubanek J, Prusak AC, Snell TW, Giese RA, Fairchild CR, Aalbersbeg W, Hay ME. Bromophycolides C-I from the Fijian red algae Callophycus densus. J. Nat. Prod. 2006; 69:731–735. [PubMed: 16724831]

Lane AL, Stout EP, Hay ME, Prusak AC, Hardcastle K, Fairchild CR, et al. Callophycoic acids and callophycols from the Fijian red alga Callophycus densus. J. Org. Chem. 2007; 72:7343–7351. [PubMed: 17715978]

Lane AL, Nyadong L, Gahlena AS, Shearer TL, Stout EP, Parry RM, et al. Desorption electrospray ionization mass spectrometry reveals surface-mediated antifungal chemical defense of a tropical seaweed. Pro. Natl. Acad. Sci. U.S.A. 2009; 106:7314–7319.

Ledlie MH, Graham NAJ, Bythell JC, Wilson SK, Jennings S, Polunin NVC, Hardcastle H. Phase shifts and the role of herbivory in the resilience of coral reefs. Coral Reefs. 2007; 26:641–653.

Leichter JJ, Stewart HL, Miller SL. Episodic nutrient transport to Florida coral reefs. Limnol. Oceano. 2003; 48:1394–1407.

Lewis SM. The role of herbivorous fishes in the organization of a Caribbean reef community. Ecol. Monographs. 1986; 56:183–200.

Mcmanus JW, Polsenberg JF. Coral-algal phase shifts on coral reefs: ecological and environmental aspects. Prog. Oceano. 2004; 60:263–279.

Mumby PJ, Steneck RS. Coral reef management and conservation in light of rapidly evolving ecological paradigms. Trends Ecol. Evol. 2008; 23:555–563. [PubMed: 18722687]

Mumby PJ. Phase shifts and the stability of macroalgal communities on Caribbean coral reefs. Coral Reefs. 2009; 28:761–773.

Nugues MM, Smith GW, Hooidonk RJ, Seabra MI, Bak RPM. Algal contact as a trigger for coral disease. Ecol. Letters. 2004; 7:919–923.

Nyadong L, Hohenstein EG, Gahlena A, Lane AL, Kubanek J, Sherrill CD, Fernandez FM. Reactive desorption electrospray ionization mass spectrometry (DESI-MS) of natural products of marine alga. Anal. Bioanal. Chem. 2009; 394:245–254. [PubMed: 19277616]

Nylund GM, Cervin G, Hermansson M, Pavia H. Chemical inhibition of bacterial colonization by Bonnemaisonia hamifera. Mar. Ecol. Prog. Ser. 2005; 302:27–36.

Nylund GM, Persson F, Lindergarth M, Cervin G, Hermansson M, Pavia H. The red alga Bonnemaisonia asparagoides regulates epiphytic bacterial abundance and community composition by chemical defence. FEMS Mico. Ecol. 2010; 71:84–93.

Ostrander GK, Armstrong KM, Knobbe ET, Gerace D, Skully EP. Rapid transition in the structure of a coral reef community: The effects of coral bleaching and physical disturbance. Proc. Natl. Acad. Sci. U.S.A. 2000; 97:5297–5302. [PubMed: 10792043]

Paul VJ, Kuffner IB, Walters LJ, Ritson-williams R, Beach KS, Becerro MA. Chemically mediated interactions between macroalgae *Dictyota* spp. and multiple life history stages of the coral Porites asteroids. Mar. Ecol. Prog. Ser. 2011; 426:161–170.

Rasher DB, Hay ME. Chemically-rich seaweeds poison corals when not controlled by herbivores. Proc. Natl. Acad. Sci. U.S.A. 2010; 107:9683–9688. [PubMed: 20457927]

Rasher DB, Stout EP, Engel S, Kubanek J, Hay ME. Macroalgal terpenes function as allelopathic agents against reef corals. Proc. Natl. Acad. Sci. U.S.A. 2011; 108:17726–17731. [PubMed: 22006333]

Ritchie KB. Regulation of microbial populations by coral surface mucus and mucus-associated bacteria. Mar. Ecol. Prog. Ser. 2006; 322:1–14.

Rogers CS, Miller J. Permanent 'phase shifts' or reversible decline in coral cover? Lack of recovery of two coral reefs in St. John, US Virgin Islands. Mar. Ecol. Prog. Ser. 2006; 306:103–114.

Schmitt TM, Hay ME, Lindquist N. Constraints on chemically mediated coevolution: multiple functions for seaweed secondary metabolites. Ecology. 1995; 76:107–123.

Smith JE, Shaw M, Edwards RA, Obura D, Pantos O, Sala E, et al. Indirect effects of algae on coral: algae-mediated, microbe-induced coral mortality. Ecol. Letters. 2006; 9:835–845.

Steinberg PD, Schneider R, Kjelleberg S. Chemical defenses of seaweeds against microbial colonization. Biodegradation. 1997; 8:211–220.

Steinberg PD, De nys R. Chemical mediation of colonization of seaweed surfaces. J. Phycol. 2002; 38:621–629.

Stout EP, Hasemeyer AP, Lane AL, Davenport TM, Engel S, Hay ME, et al. Antibacterial neurymenolides from the Fijian red alga Neurymenia fraxinifolia. Org. Letters. 2009; 11:225–228.

Takats Z, Wiseman JM, Gologan B, Cooks RG. Mass spectrometry sampling under ambient conditions with desorption electrospray ionization. Science. 2004; 306:471–473. [PubMed: 15486296]

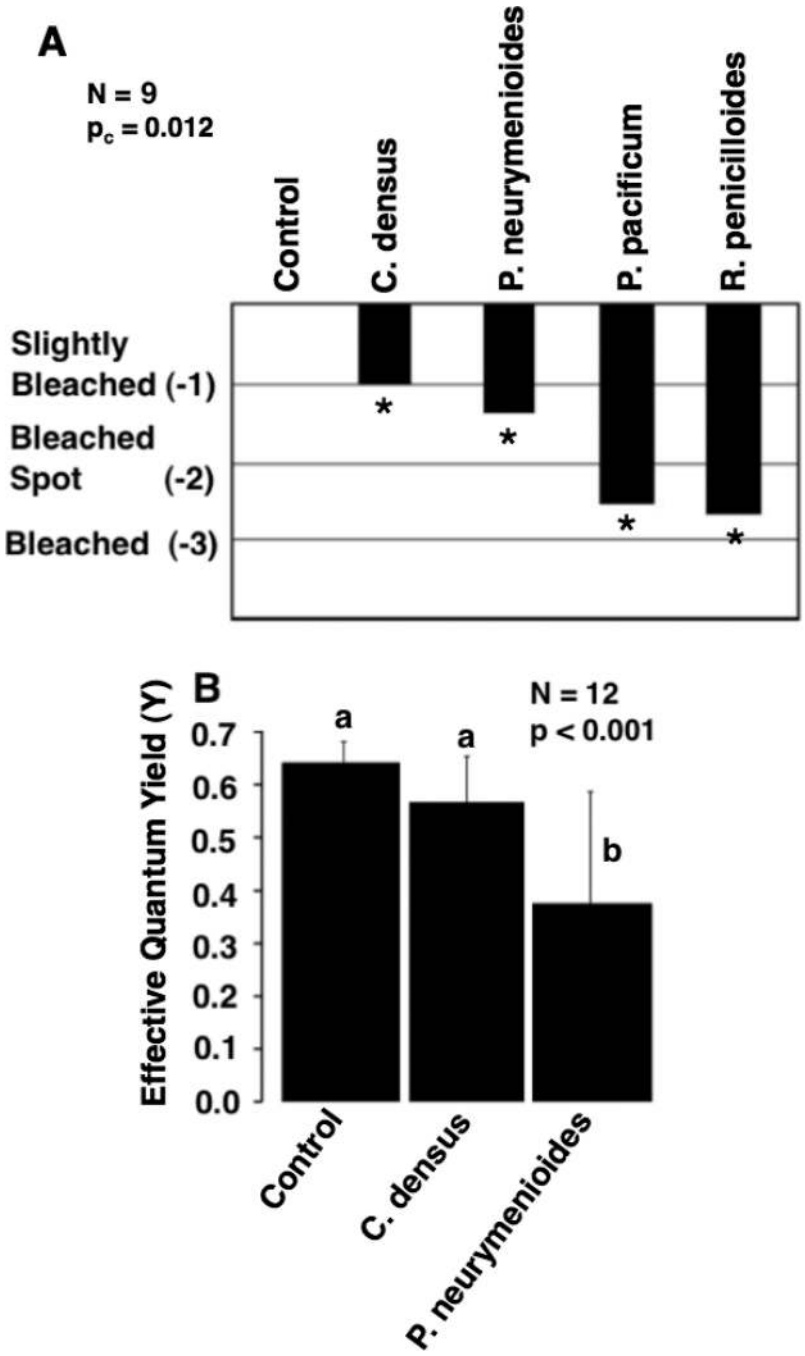

FIG. 1.

Effects of contact with whole algae (A) and crude algal extracts (B) on natural colonies of *Porites rus* ($N = 9$). Visual data were analyzed using paired sign tests (corrected $P_c = 0.012$). Photosynthetic efficiency data (Φ_{PSII}) were analyzed by a blocked ANOVA. Asterisks indicate significant differences ($P < 0.05$) between treatments and controls, and lowercase letters indicate significant groupings by *post-hoc Tukey tests*. Error bars represent standard deviation.

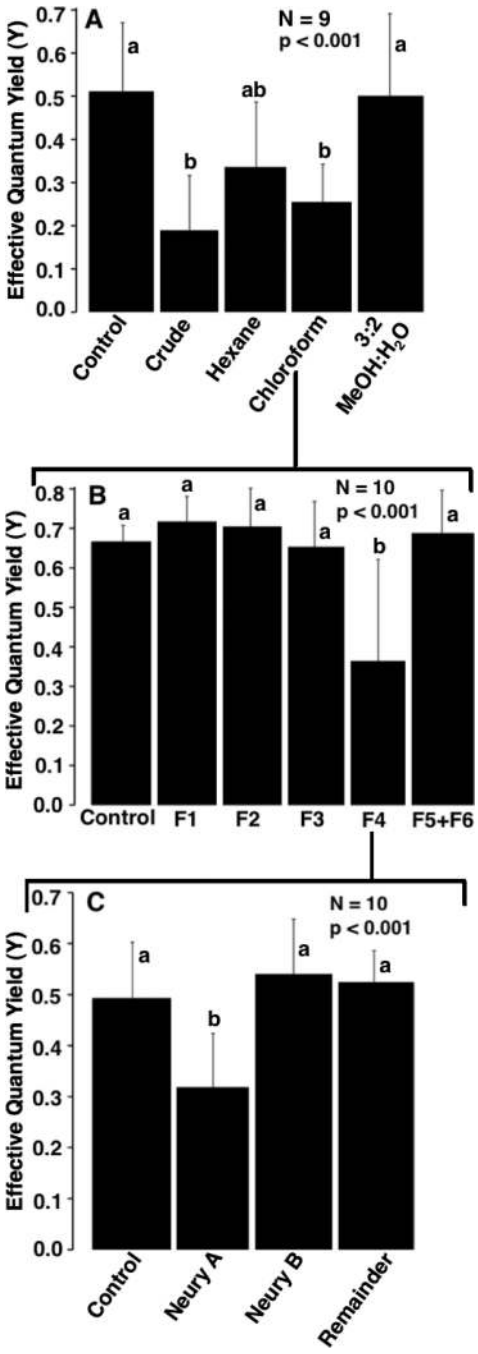

FIG. 2.

Effects of contact with chemical extracts of *Phacelocarpus neurymenioides* on natural colonies of *Porites rus* (*N* = 10). Bioassay guided fractionation began with testing of the crude extract and solvent partitions (A). Next, silica gel chromatography chloroform-soluble fractions were tested (B) followed finally by purified compounds generated from the F4 chromatography fraction (C). Photosynthetic efficiency data were analyzed by a blocked ANOVA. Lowercase letters indicate significant groupings by *post-hoc Tukey tests*. Error bars represent standard deviation.

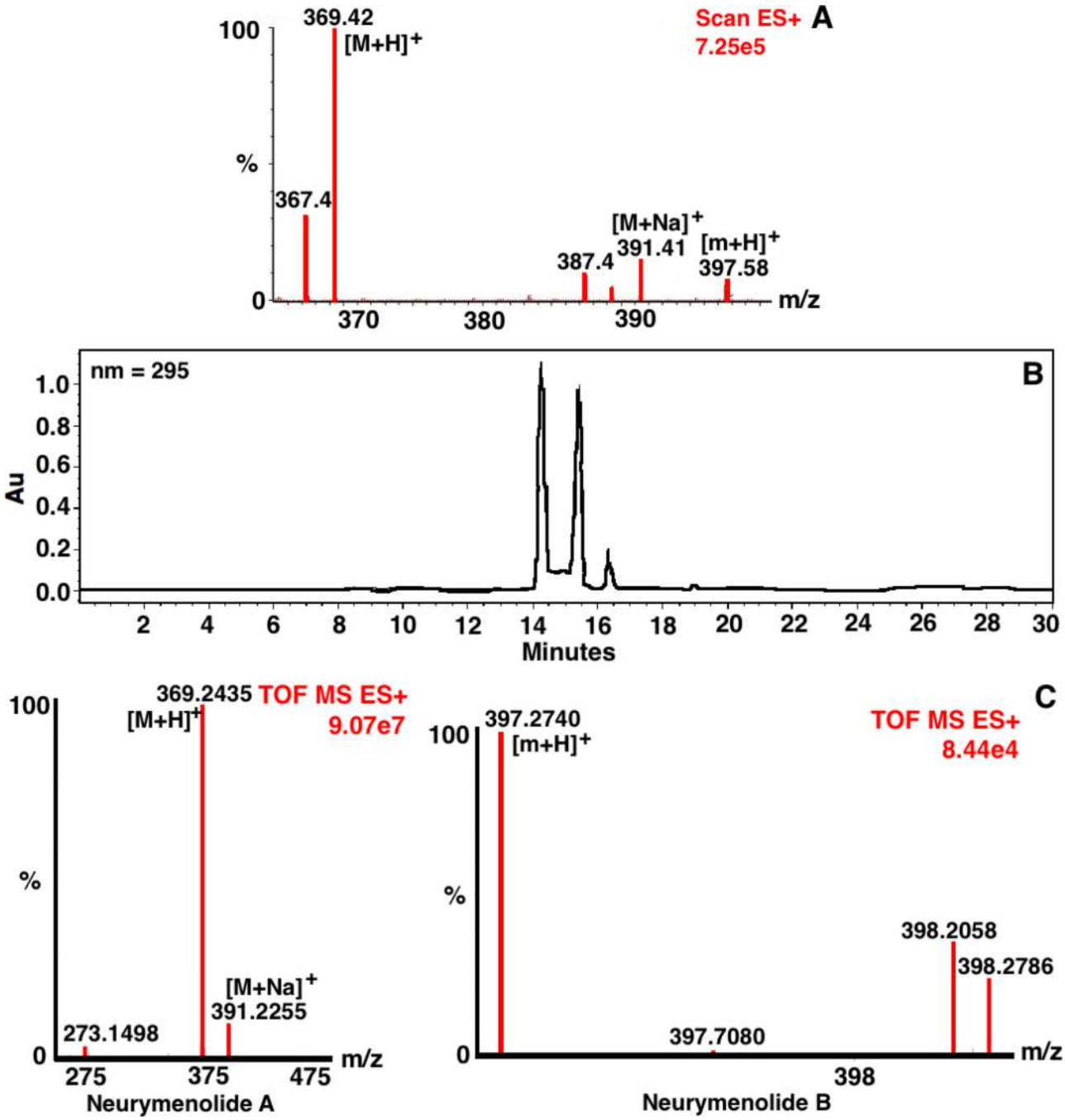

FIG. 3.

Identification of neurymenolides from extracts of *Phacelocarpus neurymenioides*. Compounds were first identified by LC-MS of the chloroform solvent partition, which shows masses matching known values for neurymenolides A (M) and B (m) (A). HPLC chromatogram from the F4 chromatography fraction showing the two associated peaks of neurymenolide A followed by the single peak of neurymenolide B (B), and accurate mass identification of both compounds using ESI-TOF (C).

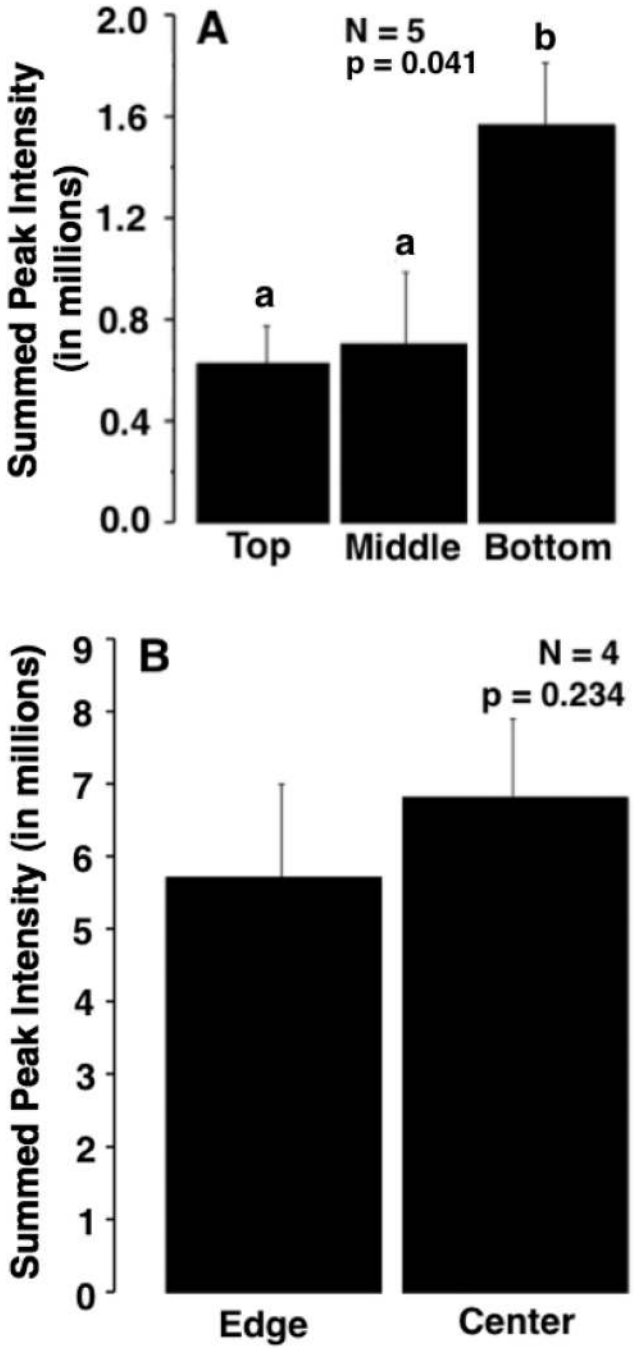

FIG. 4.

Concentration of neurymenolide A on large blades of *Phacelocarpus neurymenioides*. Differences between top, middle, and bottom portions ($N = 5$) (A) were analyzed using a blocked ANOVA. Edge and center data ($N = 4$) (B) were compared using a paired *t*-test. Lowercase letters indicate significant groupings by *post-hoc Tukey tests*. Error bars represent standard deviation.

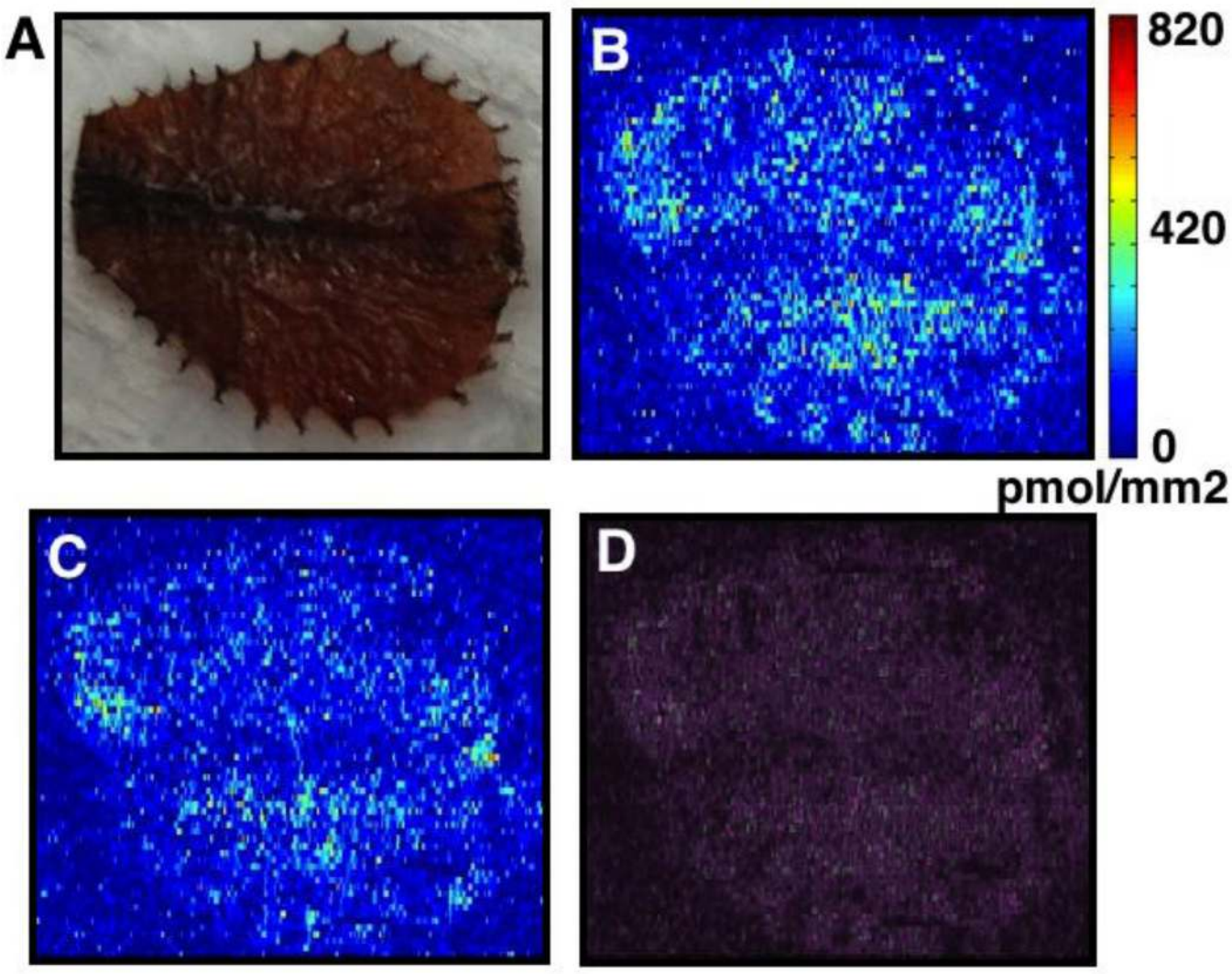

FIG. 5.

A heat-map of the concentration of neurymenolide A and its oxidative degradation products on the surface of small blades of *Phacelocarpus neurymenioides*. (A) Mass spectral data were collected using a small, live, untreated blade of *P. neurymenioides*. (B) For neurymenolide A, concentration was determined using a standard concentration curve. (C) For the degradation products the standard curve could not be applied due to possible differences in ionization rates and therefore extrapolations to concentrations could not be made. (D) An overlay of the surface distributions of neurymenolide A (pink) and oxidative degradation products (green) is purple at sites of overlap and either pink or green at sites of unique surface association.